# Green synthesis of silver nanoparticles using Randia dumetorum leaf extracts: Characterization, and assessment of biosensing activities

Kazi M.A. Haque[a*], M. Rahman[b], Md A. Saleh[a], Umer Shahzad[c], Khalid A. Alzahrani[d,e], Nahid P. Roni[a], Mohammed Muzibur Rahman[d,e], Md. M. Rahman[f]

[a]*Department of Arts & Sciences, Bangladesh Army University of Science and Technology (BAUST), Saidpur cantonment, Bangladesh*

[b]*Department of Chemistry, Hajee Mohammad Danesh Science and Technology University (HSTU), Dinajpur- 5200, Bangladesh*

[c]*International Center for Interdisciplinary Research in Sciences, The University of Lahore, Lahore, Pakistan*

[d]*Chemistry department, Faculty of Science, King Abdulaziz University, Jeddah 21589, Saudi Arabia*

[e]*Center of Excellence for Advanced Materials Research, King Abdulaziz University, Jeddah 21589, Saudi Arabia*

[f]*Abdul Kadir Mollah City College, Narsingdi, Bangladesh*

dkmah@baust.edu.bd

**Keywords:** *Green production, Randia dumetorum, Ag-NPs/GCE, Sensitivity, Thiourea sensing.*

This work emphasized the green production of silver nanoparticles employing Randia dumetorum leaf extract under alkaline conditions at room temperature. UV–Vis spectroscopy confirmed nanoparticle formation with a surface plasmon resonance band at 435 nm. SEM-EDX revealed predominantly spherical AgNPs, and XRD confirmed their crystalline nature with a mean crystallite size of 14.5 nm. In addition, an AgNP-modified glassy carbon electrode (AgNPs/GCE) was developed for thiourea sensing, exhibiting excellent sensitivity (6.329 μA $mM^{-1}$ $cm^{-2}$), linearity (0.02–0.4 μM), and low detection limits (0.0263/0.087 μM). Analysis of real water samples yielded ~99% recovery, demonstrating the sensor's reliability for practical thiourea monitoring.

## Introduction

The fusion of biotechnology with nanotechnology to provide environmentally acceptable and biosynthetic methods for the manufacture of nanomaterials has given rise to the field of bio-nanotechnology. Nanoparticles (NPs) are tiny particles that may be created in several of methods, and their diameter varies between 1 to 100 nm. Because of their size, distribution, and morphology, nanoparticles display distinct chemical, physical and thermal properties compared to bulk materials [1,2]. Nanocrystalline particles present a diverse array of applications, still more affordable and biocompatible NPs are required to improve public perceptions that "natural" ones are generally safer and better for food and medicine in the future. [3]. One significant and distinctive area of nanotechnology that is developing is the bioinspired green synthesis of NPs [4]. Silver

nanoparticles can be synthesized using several chemical and physical methods, including electrochemical processes, gamma (γ) radiation, photochemical techniques, laser ablation, and chemical reduction [5]. However, chemical reduction procedures are the most employed methods to develop nanostructures, which often involve hazardous substances including, N, N-dimethylformamide, sodium borohydride ($NaBH_4$) or hydrazine, as well as high temperatures and long periods of processing. Compared to these traditional chemical and other physical approaches, the sustainable production of nanoparticles using microorganisms [6], enzymes [7], and plant extracts [8] has significant advantages. The medicinal usefulness of biological synthesis routes is enhanced by their affordability, eco-friendliness, effortlessness for mass production, and the absence of requirements for hazardous chemicals, high pressure, high temperature, or energy [9,10]. Moreover, using plant materials is favourable than using other biochemical methods since it declines threat and the labour-intensive process of carrying on cell cultures, and it permits for a response time reduction from couple of days to several hours [11]. In addition to providing system stability, conjugating plant material elements with nanoparticles gives these NPs biocompatible functions that may be used to enhance other biological interactions.

Aqueous leaf extracts have demonstrated the ability to reduce silver ion ($Ag^+$) and rapidly cap nanosized silver (Ag) to prevent agglomerating, in addition to the utilization of bacteria, fungus, and algae [12]. The diverse therapeutic applications of metal nanoparticles, particularly silver nanoparticles (AgNPs), in addressing conditions like dermatitis, acne, and post-surgical infections make them extremely desirable [13]. Research indicates that silver exhibits less harmful effects to cells of mammals in comparison with various metallic objects, while posing a greater threat to microorganisms. Owing to their unique firmness, variety of geometrical forms, and straightforward mechanism for releasing silver contribute to the inhibition of bacterial cell growth through the generation of reactive hydrogen peroxide, AgNPs have demonstrated considerable utility in the advancement of multi-resistant therapies [14]. Additional applications of AgNPs encompass water treatment [15], agriculture [16], biomedicine [17], catalysis [18], and sensing [19].

Organic sulfur compounds containing thiourea are known to be very toxic to mammals and are hence considered a serious eco-toxin [20-22]. This chemical is known to cause cancer and allergies [23] as well as thiourea blocks nitrification in both soil and water, which throws off glucose metabolism [24,25]. Despite this, it finds extensive application in a variety of scientific and technical domains, such as analytical chemistry, agriculture, photography, the rubber industry, and electroplating [26-30]. Hence, a method to detect thiourea in wastewater and the environment needs to be adequate, sensitive, and affordable. There are now available methods for thiourea detection, such as

titrimetric [31], Raman Spectrometry [32], the HPLC method [33], and the FTIR spectrometric approach [34]. Despite the abundance of analytical methods, most of them have significant drawbacks, such as low sensitivity or selectivity or the need for expensive and complex equipment. To solve the previously identified issue with TU determination in analytical applications, quick, cheap, and easy methods are needed. In comparison to other methods, electrochemical sensors are generally considered to be the most effective because of their low cost, rapid reaction time, and high sensitivity [35,36]. The study by Iraj Jodan and colleagues on detecting TU on surfaces treated with silver and poly (alizarin) polymer was published in their journal [37]. According to this research, the LOD was determined to be 3.3 × 10− 6 $molL^{-1}$. To develop an Ag@CTSN nanocomposite and modify an electrode for TU detection, photochemically reduced silver nanoparticles were also added to chitosan. There was evidence of detecting linearity (2.0 × 10−4-3.6 × $10^{-2}$ $molL^{-1}$) and a limit of detection (LOD) of 1.8 × $10^{-5}$ $molL^{-1}$ [38,39]. In this sensor analysis, Linear Sweep Voltammetry (LSV) was selected because it provides a straightforward and reliable evaluation of the electrocatalytic oxidation behavior of thiourea at the AgNPs/GCE interface. The well-defined oxidation peak and excellent analytical performance obtained by LSV, including a low detection limit and high sensitivity, were sufficient to validate the sensing capability of the developed electrode. Although pulse techniques such as differential pulse voltammetry (DPV), square-wave voltammetry (SWV), and amperometry may further enhance sensitivity by reducing capacitive current, these techniques will be explored in future studies to further optimize the sensor performance

*Randia dumetorum*, a member of the Rubiaceae family, is a renowned herbal medicinal tree. The foliage of Randia dumetorum comprises iridoid-10-methylixoside, while the root bark carries the triterpene 1-keto-3-hydroxyoleanane. Researchers mentioned that randianin, triterpenoid glycosides, and glycosides are all present in *Randia dumetorum*. Moreover, various saponins, including dumentoronin A, B, C, D, E, and F etc have also been found in this member of Rubiaceae. It treats abscesses, ulcers, inflammation, wounds, tumors, skin disorders and has an antibacterial impact [40].

This study outlines the green manufacturing of silver nanoparticles which involves several steps such as, selection of nontoxic solvent medium, an environmentally sustainable reducing substance and harmless chemicals to ensure environment protection and nanoparticles stability [41]. In recent years, multiple processes are being implemented in order to produce nanosized silver particles in an environmentally friendly manner [42] in which different disaccharides, polysaccharides and leaf extracts are most commonly used as reducing materials and water is considered as a solvent medium [43,44]. For instance, researchers outlined the green synthesis of AgNPs applying starch and glucose as a stabilizing component and a

reductant, respectively. The separation of synthesized nanoparticles could be carried out effectively due to the weak binding interactions between the resulting silver nanoparticles and starch [45]. *Plectranthus amboinicus* leaf extract was recently employed to synthesize silver nanoparticles (AgNPs) in a green path [46]. Additionally, for the green production of AgNPs, the extract of *Solanum torvum* has been used in another work [47]. The evaluation of these biosynthesized nanoparticles demonstrated their exceptional antibacterial properties against different types of bacteria. Also, it has been seen that *Taxus baccata* extracts can be used as reducing, capping, and stabilizing agents to make silver nanoparticles with the size of less than 100 nm in a simple, effective, and environmentally benign way [44].

The present research work mainly focuses on the synthesis of AgNPs employing the leaf extract of *Randia dumetorum* which serve as both a reductant and capping agent. The characterization of the synthesized silver nanoparticles has been carried out by different spectroscopic and microscopic methods including FTIR spectroscopy, UV-Vis spectroscopy, Scanning Electron Microscope (SEM) with EDX analysis in order to verify the successful synthesis of AgNPs. In addition, to develope a selective TU sensor, this research aims to create a Ag-nanoparticle sensing substrate that might be used on a GCE. The constructed sensor probe was put through its paces in terms of sensitivity, detection range, reaction time, repeatability, and stability over time, among many other things. Results were deemed positive and promising for the acquired parameters. Upon careful analysis of actual bio-samples used for validation and reliability testing, the results were adequate and satisfactory. The use of carbon nanotubes conjugated with metal oxides could provide a dependable real-time monitoring sensor probe, suggesting that this strategy could be a viable option for enhancing electrochemical sensors.

## Materials and Methods

**2.1 Plant collection:** The study's medicinal plant was collected in March 2024 from Sreemangal area of Bangladesh's Sylhet division. The herbal plant *Randia dumetorum***,** also known as Monkata in Bangladesh, was identified and brought to the lab for further processing.

**2.2 Chemicals:** The following analytical grade chemicals were purchased from Merck: potassium ferrocyanide ($K_4[Fe(CN)_6]$), dipotassium hydrogen phosphate ($K_2HPO_4$), thiourea, potassium ferricyanide ($K_3[Fe(CN)_6]$), sodium hydroxide (NaOH), hydrochloric acid (HCl), and potassium dihydrogen phosphate ($KH_2PO_4$). We used deionized water to produce solutions without further purifying the other ingredients. The compounds that were considered were of analytical quality. Salts of $KH_2PO_4$ and $K_2HPO_4$ were used to make a phosphate buffer solution (PBS) with a concentration of 0.1 M while the pH of the solution was adjusted using sodium hydroxide (NaOH) and hydrochloric acid (HCl).

**2.3 Preparation of leaf extract:** Prior to sun drying, plant leaves were thoroughly cleansed

with distilled water. The samples were kept in clearly marked, airtight plastic containers until the leaves had fully dried and were ground up using a porcelain mortar and pestle [48]. After weighing 3.33 g of powdered leaves, 200 mL of distilled water was added, and the resulting mixture was heated about 20 to 30 minutes at 58-60°C in a water bath. Subsequently, the filtration of the mixture was carried out via Whatman filter paper, yielding filtrate which is light brown in color. The extracts were then utilized further to synthesize AgNPs.

**2.4 Synthesis of silver nanoparticles from liquid plant extracts:** Typically, 200 mL of 20 mM $AgNO_3$ was combined to 50 mL of the aqueous leaf extracts, which were quantified and then reacted. To maintain basic medium, 10 mL of 0.025M NaOH solution was added to it. The resulting mixture was settled 24 hours before separation by centrifuging them. After the transparent filtrates were decanted, the settling layer was centrifuged in order to collect the nanoparticles followed by drying at room temperature and stored in a designated 5 mL plastic sample vial.

**2.5 Fabrication of working electrode (GCE):** The working electrode sensor, a vital component of the proposed sensor, was created by modifying a glassy carbon electrode (GCE) with Ag-nanoparticles. A thin coating of an ethanol-based Ag-nanoparticle slurry was applied to a clean GCE surface and then let to dry in the lab's ambient conditions to create the working electrode. The GCE's nanocomposite layer was given a little Nafion adhesive, which made it more stable and extended the electrode's working duration. Then, it was let dry out at room temperature. The Metrohm Autolab Potentiostate was used for all electrochemical studies. The three-electrode setup in an electrochemical cell consisted of a GCE (working electrode), an Ag/AgCl (3.0 M KCl) (reference electrode), and a Pt wire (counter electrode).

## Result and Discussion

### 3.1 UV-Vis spectroscopy analysis

The synthesis of silver nanoparticles (AgNPs) through the reduction of silver nitrate ($AgNO_3$) utilizing the leaf extracts of *Randia dumetorum* has been demonstrated by the observed color change in the solution. Then, UV-Vis spectroscopy was used to characterize the produced nanoparticles in which the characteristics maxima was recorded at about 435 nm [48] (**Figure 1**).

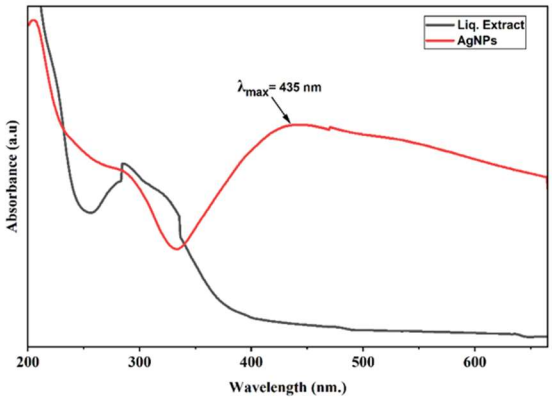


**Figure 1.** UV-Vis Spectroscopic spectra of green synthesized silver nanoparticles and liquid extract.

The spectrum should be compared with the spectrum of the leaves extract to identify the surface plasmon resonance.

### 3.2 FTIR analysis

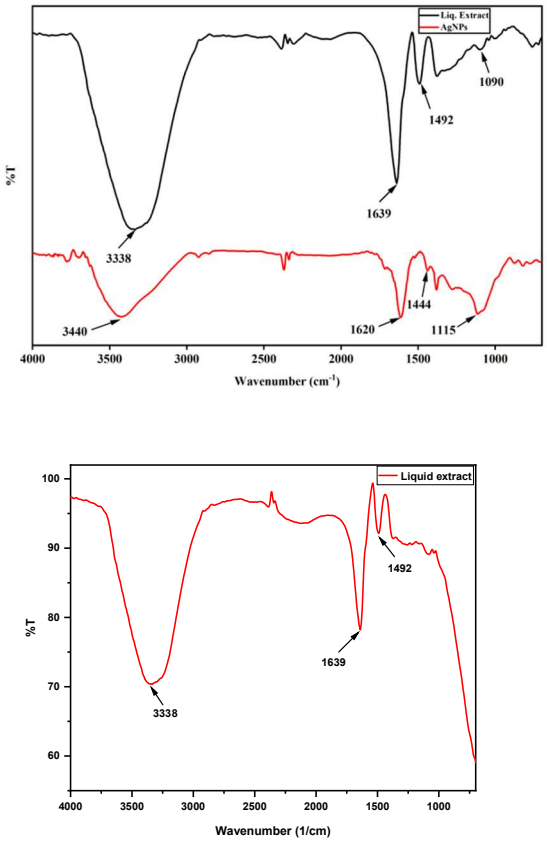


**Figure 2.** Merged FT-IR spectra of green synthesized silver nanoparticles associated possible capping agents and liquid extract.

**Figure 2a** illustrates various absorption bands in the FTIR spectrum of the obtained AgNPs. The absorption band at 3440 $cm^{-1}$ refers to have surface -OH groups, at 1620 $cm^{-1}$ the characteristic peak of the carbonyl functional (C=O) group indicates having a somewhat organic reducing agent, the band frequency at 1438 $cm^{-1}$ is attributed to aromatic C=C vibrations, the vibrational frequency at 1115 $cm^{-1}$ assigned to C-O single bond [47]. Comparing the two spectra, Ag–O was observed in the AgNPs spectrum (**Figure 2a**), implying the presence of silver nanoparticles formation along with different capping agents. FTIR analysis identified the distinct functional groups possibly the cause of reducing $AgNO_3$, capping as well as effective stability of the newly synthesized silver nanoparticles.

### 3.3 SEM-EDX analysis

The SEM-EDX analysis confirmed the successful green synthesis of AgNPs. This analysis exhibited the nanoparticles to be rough-edged crystalline. The diameter of the particles was determined using the scale bar at the bottom left of the **Figure 3a** and it was approximately 18nm. Elemental analysis was confirmed by the EDX spectrum, which displayed a significant characteristic signal of silver, carbon and oxygen at about 3 keV (**Figure 3b**). The existence of signals for carbon and oxygen was observed which are might be due to the capping agents.

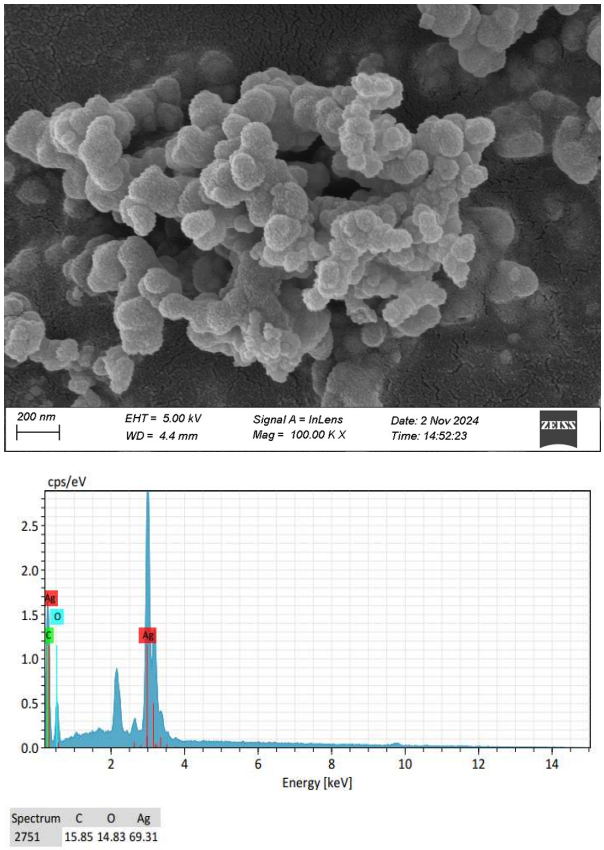


**Figure 3.** SEM-EDX images of silver nanoparticles

### 3.4 X-ray diffraction (XRD) pattern analysis

The X-ray diffraction (XRD) pattern of the synthesized AgNPs revealed the presence of noteworthy diffraction peaks at 2θ values of about 38.04°, 44.18°, 64.46° and 77.5° (figure 4). The observed peaks align with the ((111), (200), (220), and (311)) (JCPDS No. 04-0783) of face-centered cubic (fcc) silver nanoparticles. Using the Debye-Scherrer equation ($D = \frac{K\lambda}{\beta Cos\theta}$), the mean crystal size was obtained around 14.5 nm. The sharp and strong peaks represent the nanoparticles have a high degree of crystallinity. The absence of any other peak proves the purity of the silver nanoparticles.

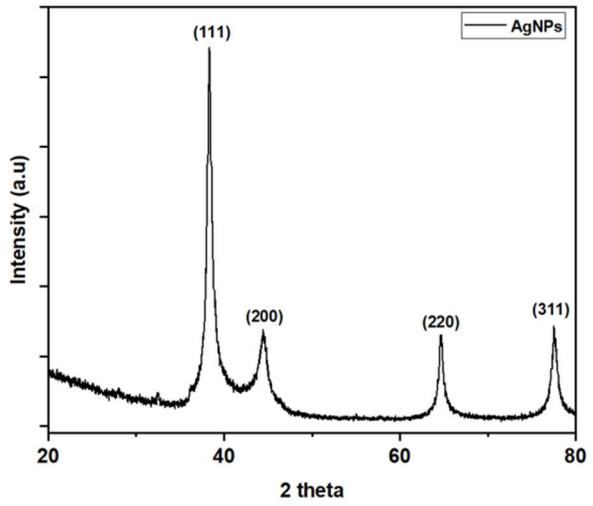


**Figure 4**. X-Ray Diffraction pattern of silver nanoparticles.

### 3.5 Electrochemical detection of thiourea with AgNP coated GCE

The concentration of thiourea varied between 0.07 µM and 0.40 µM, and its electrochemical behavior was analyzed using cyclic voltammetry (CV). As the concentration increased, a notable enhancement in the current response was observed, indicating a proportional relationship between thiourea concentration and electrochemical activity within this range. This trend suggests that higher thiourea concentrations result in an increased number of electroactive species participating in the redox process at the electrode surface. The CV curves exhibited consistent shifts in peak current intensity, confirming the sensitivity of the method to changes in thiourea levels. These results highlight the effectiveness of CV for monitoring thiourea concentrations in a controlled system (**Figure 5a).** Electrochemical oxidation tests of thiourea were carried out in a 0.1 M phosphate-buffered saline (PBS) electrolytic solution having 7.5 pH. The as-prepared electrode was analyzed using cyclic voltammetry (CV) and linear sweep voltammetry (LSV).

The cyclic voltammograms of Ag-NPs/GCE recorded in the presence of thiourea (0.07–0.40 µM) exhibit two anodic peaks and one cathodic peak, indicating a multi-step electrochemical oxidation process. The first anodic peak is attributed to the initial oxidation of thiourea into intermediate species such as formamidine disulfide via a two-electron/two-proton transfer process. The second anodic peak is associated with the further oxidation of these intermediates and/or strongly adsorbed sulfur-containing species formed on the Ag-NPs surface. The presence of Ag nanoparticles facilitates adsorption and electron transfer, thereby enhancing the oxidation kinetics of thiourea.

The cathodic peak corresponds to the reduction of oxidized surface species generated during the forward scan, likely involving

reversible Ag–S/Ag-oxide related species. Among the two anodic responses, the first oxidation peak shows a more pronounced and linear increase with thiourea concentration, indicating its suitability as the analytical signal for electrochemical sensing. The progressive increase in peak current with increasing thiourea concentration confirms the excellent electrocatalytic activity of Ag-NPs/GCE toward thiourea oxidation.

Voltammograms recorded at a scan rate of 100 mV/s for bare glassy carbon electrodes (GCE), AgNPs/GCE without thiourea, and AgNPs/GCE with thiourea are presented in **Figure 5b**. Thiourea, at a concentration of 0.1 M, was used as the test analyte. The AgNPs/GCE electrode exhibited a faster electrochemical activity at the anode equated to the unchanged GCE over the identical potential window. The AgNPs/GCE electrode showed a distinct anodic peak with a substantial increase in current at 0.4 V, which is notably lower in contrast to the anodic peaks of the other electrodes, occurring at approximately 0.092 V. The AgNPs/GCE electrode also demonstrated enhanced oxidation currents and increased capacitance compared to the bare GCE and unmodified GCE, as shown in **Figure 5b**. This higher capacitive current can be attributed to the increased surface area provided by the silver nanoparticles (AgNPs/GCE). The enhanced surface area not only boosts catalytic activity but also improves the interaction between the analyte and the electrocatalyst, creating numerous new active sites for the reaction to occur. We conducted electrochemical tests to see how well the Ag-NPs coating held up on a glassy carbon electrode that had been bonded with Nafion. In a solution of potassium hexacyanoferrate(II) ($K_4[Fe(CN)_6]$) with a concentration of 0.1 M, the electrode that had been coated with nanocomposite material was examined. There was minimal to no performance degradation after 50 CV cycles, as seen in **Figure 5c**. This bodes well for the electrode's stability and its potential for dependable examination of additional chemicals.

To investigate the influence of modifying scan rates (10–500 mV/s) on the electrochemical performance of the AgNPs/GCE electrode, a solution containing 0.1 M of $K_3[Fe(CN)_6]$ and $K_4[Fe(CN)_6]$ in 0.1 M PBS was used. **Figure 5d** shows that the peak currents increase proportionally with the scan rate, indicating a diffusion-controlled reaction mechanism. This linear relationship is further confirmed by the regression equations derived from the plot of the square root of the scan rate versus peak current in Figure 5(e):

$$\mathbf{I_{pa} = 300.89x - 443.04 \ (R^2 = 0.98)}$$

$$\mathbf{I_{pc} = y = 92.33x + 165.64 \ (R^2 = 0.98)}$$

The data suggest that the AgO/GCE electrode operates on a diffusion-controlled mechanism, as evidenced by the direct proportionality between the square root of the scan rate and the peak current.

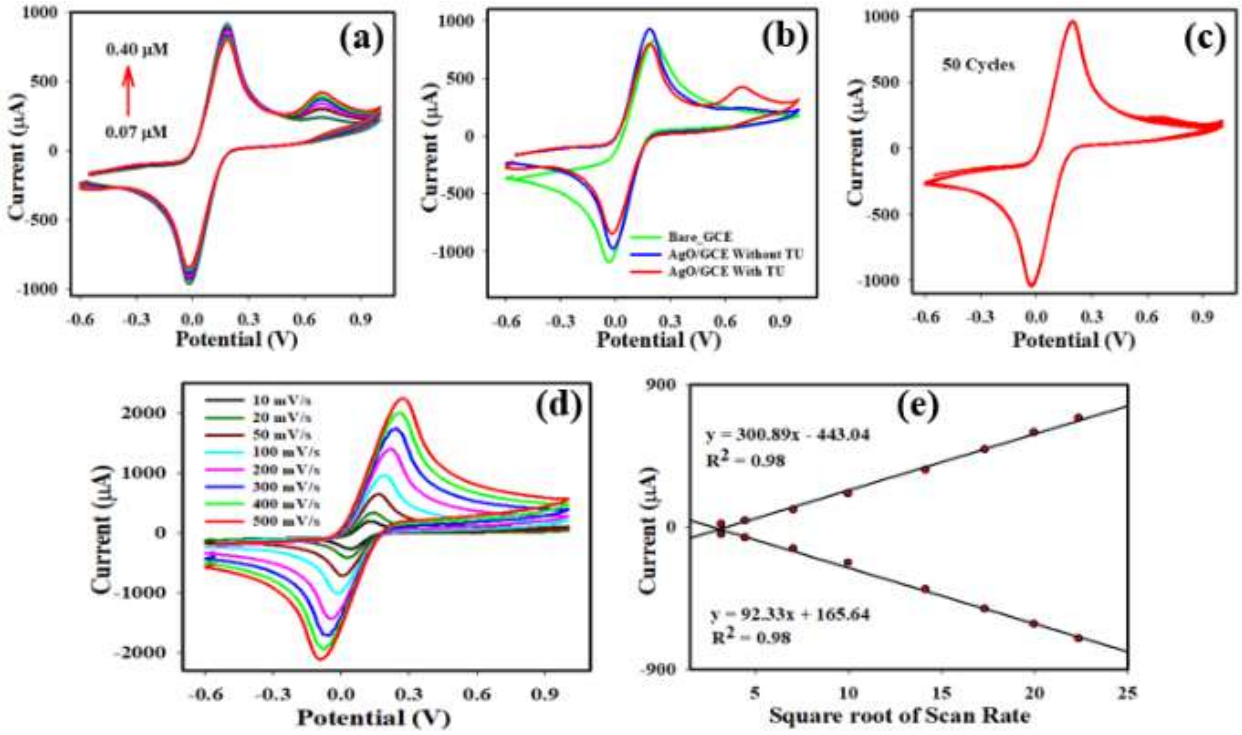


**Figure 5.** Electrochemical Characterization of Ag-NPs/GCE. (a) Cyclic Voltammogram illustrating concentration variations from 0.07 µM and 0.40 µM demonstrating sensitivity and detection capability (b) Control experiment containing Bare and coated GCEs measured by CV (c) Stability Assessment of Ag-NPs/GCE measured by cyclic voltammetry, indicating reliable performance over time with 50 cycles at scan rate of 100 mV/s; (d) CV Scan Rate Analysis from 10 mV/s to 500 mV/s, providing insights into the kinetics of the electrochemical process; (e) Regression Line for scan rate data, facilitating the understanding of diffusion-controlled processes in the composite electrode.

The oxidation of thiourea (TU) proceeds through a one-electron transfer process, resulting in the formation of a C,C'-dithiodiformamidinium ion (III). This intermediate further reacts to produce a dimerized product, formamidine disulfide (FDS), which is subsequently reduced during the reverse scan. In the voltammograms of AgNPs/GCE, a single anodic peak and its corresponding cathodic peak are observed. These peaks are associated with the conversion of thiourea into the C,C'-dithiodiformamidinium ion (III) and its reverse transformation. Based on these observations, the proposed oxidation mechanism can be represented by the following scheme (**Scheme 1**) [38].

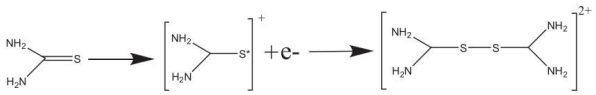


**Scheme 1.** Detection mechanism of TU with AgNPs/GCE electrode.

Linear sweep voltammetry (LSV) was conducted to assess the performance of the newly prepared AgNPs/GCE for thiourea (TU) detection. The study was performed in a 0.1 M PBS solution across TU concentrations ranging from 0.02 to 0.40 µM, asserting a fixed scan rate of 100 mV/s. As depicted in **Figure 6a**, the anodic current increased with each successive addition of thiourea, demonstrating the electrocatalyst's ability to detect thiourea effectively. This rise in oxidation current is attributed to the sensor electrode's excellent

charge detection properties and the availability of mobile electrons.

A linear relationship between peak current (Ipa) and TU concentration was observed over the entire concentration range, described by the equation:

$$\mathbf{I_{pa} = 190.29x + 65.454\ [TU]}$$

This equation shows a high coefficient of determination ($r^2 = 0.98$), as depicted in **Figure 6b**. The LOD was computed applying Equation (3):

$$\mathbf{LOD = 3\sigma/m} \qquad \mathbf{(3)}$$

where the blank electrolyte standard deviation is denoted by σ and m is the calibration curve slope.

The calculated LOD value of 0.02638 µM is comparable to, or even better than, values obtained with other electrodes, as detailed in **Table 1**. The AgNPs/GCE electrode shows significant sensing capability due to cheapness, ease of fabrication, and minimal preparation requirements, making it a potential alternative to more complex and expensive materials.

The AgNPs/GCE probe does not consistently provide reliable electrochemical responses to TU solely by adjusting the pH of the PBS electrolyte. Therefore, optimizing the pH is crucial for enhancing the sensor's electrocatalytic performance. This was remedied by testing the sensor in buffer solutions having pH values between 5.7 and 8.0. Electrochemical measurements of 0.1 M TU across a potential range of -1 to +1.8 V are presented in **Figure 6c,d**, demonstrating the pH dependence of the sensor's response. The optimal performance of the AgNPs/GCE electrode was observed at pH 7.5, which was subsequently used in all experiments. To validate the sensor's reliability, repeatability and selectivity studies were evaluated. For repeatability, five LSV tests were conducted with the AgNPs/GCE electrode in BS (pH 7.5), detecting TU concentrations as shown in **Figure 6e**.

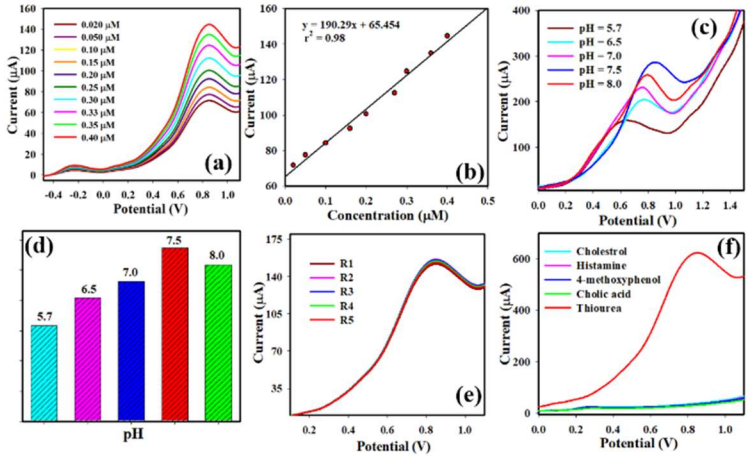


**Figure 6.** (a) LSV of Ag-NPs/GCE with 0.020 to 0.40 µM concentration assortment; (b) Peak current vs thiourea concentration; calibration curve. (c) LSV response for pH optimization in 0.1 M PBS across a range of pH values (5.7-8.0), assessing the effect of pH on the electrochemical performance; (d) Bar Chart summarizing the results of pH Optimization, indicating the optimal conditions for enhanced sensor performance. (e) Find the LSV using a single electrode over the course of five repeated measurements (f) Selectivity measurement LSV graph highlighting the sensor's ability to differentiate thiourea from potential interferents.

Selectivity was assessed by LSV electrochemical technique with interfering substances such as cholesterol, histamine, and 4-methoxyphenol (4-MP), each introduced at concentrations five times higher than TU in 0.1 M PBS at pH 7.5. The interfering compounds produced minimal or negligible voltametric signals, while the addition of TU to the reaction mixture resulted in a significant increase in current, as depicted in **Figure 6f**. These findings confirm the high selectivity and repeatability of the AgNPs/GCE sensor for thiourea detection.

**Table 1**. Comparative study of the newly prepared Ag-NPs/Nafion/GCE against thiourea detection with other electrode materials.

| Modified Electrode | Technique | LOD (µM) | Linear range | Sensitivity ($mAmM^{-1}$ $cm^{-2}$ ) | References |
|---|---|---|---|---|---|
| AuE | CV | $5.0 \times 10^{-5}$ $molL^{-1}$ | $5.0 \times 10^{-5}$ -$1.0 \times 10^{-3}$ | - | [49] |
| CuO/Cu | CV | - | 1000–8000 µM | 1.30 | [50] |
| Pencil graphite electrode | SWV | $1.29 \times 10^{-6}$ $molL^{-1}$ | $6.3 \times 10^{-6}$ -$3.0 \times 10^{-5}$ $molL^{-1}$ | - | [51] |
| Y/Co-MWCNT | LSV | $2.83 \times 10^{-8}$ mM | 0.70-3.1nM | 5.8544 | [52] |
| **Ag-NPs/Nafion/GCE** | **LSV** | **0.02638 µM** | **0.07-0.40 µM** | **6.329 µA$mM^{-1}cm^{-2}$** | **This Work** |

### 3.5.1 Real Sample Assessment:

The AgNPs/GCE sensor, in conjunction with electrochemical techniques and the conventional addition method, was able to detect thiourea in samples of seawater, well water, and tap water supply. Each concentration measurement was performed in triplicate, and the average current values were used to determine the thiourea concentrations. The results, summarized in **Table 2**, show relative standard deviations below 1% and recovery rates of approximately 99%. These outcomes are consistent with the standard calibration curve method, confirming the sensor's accuracy. These findings highlight the potential of the Ag-NPs/GCE sensor for practical applications in real-world sample analysis.

**Table 2.** Comparison of proposed sensor Ag-NPs/GCE for TU detection with already published work

| Real Samples | Added TU conc. (µM) | Measured TU Conc. by Ag-NPs/GCE (µM) | | | Average Recovery | RSD (%) (n=3) |
|---|---|---|---|---|---|---|
| | | R1 | R2 | R3 | | |
| Sea water | 0.40 | 0.4017 | 0.3958 | 0.3997 | 99.76 | 0.752 |
| Well water | 0.40 | 0.3983 | 0.4004 | 0.3980 | 99.72 | 0.328 |
| Tap water | 0.40 | 0.3944 | 0.3967 | 0.4026 | 99.48 | 1.06 |

## Conclusion

In this study, silver nanoparticles (AgNPs) have been successfully synthesized using an eco-friendly approach involving the leaf extract of *Randia dumetorum*. The characterization techniques, such as UV-Vis spectroscopy, FTIR,

SEM-EDX, and XRD, confirmed the formation of spherical, rough-edged crystalline AgNPs, measuring an average size of around 14.5 nm. In order to circumvent the intricacy of the traditional method as a potential biosensing material, a recently created Ag-NPs/GCE electrochemical sensor was employed for the specific identification of TU. To determine the peak response for each known TU concentration, we employed CV and LSV electrochemical methods. In comparison to prior studies, the AgNPs-modified GCE electrode performed significantly better, with a linear range of 0.02-0.4 μM and a limit of detection of 0.0263 μM. Consequently, the results of this investigation indicate that the created sensor might be useful for detecting TU in various real-world water samples. Contributing to the protection of human health and the preservation of the environment, this study marks a significant step toward developing a chemical sensor for recognizing harmful contaminants utilizing AgNPs. The findings reveal that AgNPs obtained by using *Randia dumetorum* possess substantial possibilities for using in environmental applications, presenting a sustainable alternative to traditional nanoparticle synthesis techniques.

## 5. Acknowledgment

The authors express their sincere gratitude to the Ministry of Science and Technology (MoST), Bangladesh. Center of Excellence for Advanced Materials Research for their technical supports and performed the sensor applications.

## References

[1] Khan I, Saeed K, Khan I. Nanoparticles: Properties, applications and toxicities. Arabian Journal of Chemistry 2019;12(7):908-931.

[2] Ajitha B, Ashok Kumar Reddy Y, Sreedhara Reddy P. Green synthesis and characterization of silver nanoparticles using Lantana camara leaf extract. Materials Science and Engineering: C 2015;49:373-381.

[3] Greathead H. Plants and plant extracts for improving animal productivity. Proceedings of the Nutrition Society 2003;62(2):279-290.

[4] Shankar S, Rai A, Ahmad A, Sastry M. Rapid synthesis of Au, Ag, and bimetallic Au core–Ag shell nanoparticles using Neem (Azadirachta indica) leaf broth. Journal of Colloid and Interface Science 2004;275(2):496-502.

[5] Iravani S, Korbekandi H, Mirmohammadi SV, Zolfaghari B. Synthesis of silver nanoparticles: chemical, physical and biological methods. Res Pharm Sci. 2014;9(6):385-406

[6] Narayanan K, Sakthivel N. Biological synthesis of metal nanoparticles by microbes. Advances in Colloid and Interface Science 2010;156(1-2):1-13.

[7] Schneidewind H, Schüler T, Strelau K, Weber K, Cialla D, Diegel M, Mattheis R, Berger A, Möller R, Popp J. The morphology of silver nanoparticles prepared by enzyme-induced reduction. Beilstein Journal of Nanotechnology 2012;3:404-414.

[8] Sulaiman G, Mohammed W, Marzoog T, Al-Amiery A, Kadhum A, Mohamad A. Green synthesis, antimicrobial and cytotoxic effects of silver nanoparticles using Eucalyptus chapmaniana leaves extract. Asian Pacific Journal of Tropical Biomedicine 2013;3(1):58-63.

[9] Vimalanathan AB, Tyagi V, Rajesh A, Devanand P, Tyagi MG. Biosynthesis of silver nanoparticles using Chinese white ginseng plant root Panax ginseng. Int J Pharm Sci Res. 2013;4(7):2716-2725.

[10] Kouvaris P, Delimitis A, Zaspalis V, Papadopoulos D, Tsipas S, Michailidis N. Green synthesis and characterization of silver nanoparticles produced using Arbutus Unedo leaf extract. Materials Letters 2012;76:18-20.

[11] Kumar V, Yadav S. Plant-mediated synthesis of silver and gold nanoparticles and their applications. Journal of Chemical Technology & Biotechnology 2008;84(2):151-157.

[12] Ansar S, Tabassum H, Aladwan N, Naiman Ali M, Almaarik B, AlMahrouqi S, Abudawood M, Banu N, Alsubki R. Eco friendly silver nanoparticles synthesis by Brassica oleracea and its antibacterial, anticancer and antioxidant properties. Scientific Reports 2020;10(1):.

[13] Contreras EQ. Investigating the biological impacts of nanoengineered materials in Caenorhabditis elegans and in vitro. Rice University; 2012.

[14] Ojemaye M, Okoh S, Okoh A. Silver nanoparticles (AgNPs) facilitated by plant parts of Crataegus ambigua Becker AK extracts and their antibacterial, antioxidant and antimalarial activities. Green Chemistry Letters and Reviews 2020;14(1):51-61.

[15] Zhao Y, Fan M, Zhou W, Li Y, Wang Y, Xiu Z, Gao B. Speciation, controlling steps and pathways of silver release from the sludge generated from coagulation of wastewater spiked with silver nanoparticles. Chemosphere 2021;282:131093.

[16] Khan J, Chandra J, Xalxo R, Korram J, Satnami M, Keshavkant S. Amelioration of Ageing Associated Alterations and Oxidative Inequity in Seeds of Cicer arietinum by Silver Nanoparticles. Journal of Plant Growth Regulation 2020;40(3):1341-1351.

[17] Akintelu S, Olugbeko S, Folorunso A, Oyebamiji A, Folorunso F. Potentials of phytosynthesized silver nanoparticles in biomedical fields: a review. International Nano Letters 2021;11(3):273-293.

[18] Ajitha B, Ahn C, Yadav P, Reddy Y. Silver nanoparticle embedded polymethacrylic acid/ polyvinylpyrrolidone nanofibers for catalytic application. Journal of Environmental Chemical Engineering 2021;9(5):106291.

[19] Jiang C, Bai Z, Yuan F, Ruan Z, Wang W. A colorimetric sensor based on Glutathione-AgNPs as peroxidase mimetics for the sensitive detection of Thiamine (Vitamin B1). Spectrochimica Acta Part A: Molecular and Biomolecular Spectroscopy 2022;265:120348.

[20] Safavi A, Ahmadi R, Mahyari F, Tohidi M. Electrocatalytic oxidation of thiourea on graphene nanosheets–Ag nanoparticles hybrid ionic liquid electrode. Sensors and Actuators B: Chemical 2015;207:668-672.

[21] Rahman M, Ahmed J, Asiri A. Thiourea sensor development based on hydrothermally prepared CMO nanoparticles for environmental safety. Biosensors and Bioelectronics 2018;99:586-592.

[22] Subhan M, Jhuma S, Saha P, Ahmed J, Asiri A, Rifat T, Raihan T, Azad A, Rahman M. Photocatalysis, enhanced anti-bacterial performance and discerning thiourea sensing of Ag2O·SnO2·TiO2 hetero-structure. Journal of Environmental Chemical Engineering 2020;8(4):104051.

[23] Sahu S, Rani Sahoo P, Patel S, Mishra B. Oxidation of thiourea and substituted thioureas: a review. Journal of Sulfur Chemistry 2011;32(2):171-197.

[24] Chen C, Zhao D, Sun J, Yang X. A dual-mode signaling response of a AuNP-fluorescein based probe for specific detection of thiourea. The Analyst 2016;141(8):2581-2587.

[25] Smyth M, Osteryoung J. Determination of some thiourea-containing pesticides by pulse voltammetric methods of analysis. Analytical Chemistry 1977;49(14):2310-2314.

[26] Spataru N, Spataru T, Fujishima A. Voltammetric Determination of Thiourea at Conductive Diamond Electrodes. Electroanalysis 2005;17(9):800-805.

[27] Jodan I, Wantala K, Amini N, Shahmoradi B, Ghaslani M, Lee S, Yang J, Puttaiah S. Fabrication of a sensitive electrochemical sensor based on Ag nanoparticles and alizarin yellow polymer: Application to the detection of an environmental pollutant thiourea. Korean Journal of Chemical Engineering 2020;37(9):1609-1615.

[28] Abbasi S, Khani H, Gholivand M, Naghipour A, Farmany A, Abbasi F. A kinetic method for the determination of thiourea by its catalytic effect in micellar media. Spectrochimica Acta Part A: Molecular and Biomolecular Spectroscopy 2009;72(2):327-331.

[29] Wang W, Dong Z, Yang C, Li G, Tse Y, Leung C, Ma D. An iridium(III) complex-based chemosensor for

the detection of thiourea in living cells. Sensors and Actuators B: Chemical 2017;251:374-379.

[30] Abbasi S, Khani H, Hosseinzadeh L, Safari Z. Determination of thiourea in fruit juice by a kinetic spectrophotometric method. Journal of Hazardous Materials 2010;174(1-3):257-262.

[31] Amin D. Determination of thiourea, phenylthiourea and allythiourea with iodine. The Analyst 1985;110(2):215.

[32] Bowley H, Crathorne E, Gerrard D. Quantitative determination of thiourea in aqueous solution in the presence of sulphur dioxide by Raman spectroscopy. The Analyst 1986;111(5):539.

[33] Rethmeier J, Neumann G, Stumpf C, Rabenstein A, Vogt C. Determination of low thiourea concentrations in industrial process water and natural samples using reversed-phase high-performance liquid chromatography. Journal of Chromatography A 2001;934(1-2):129-134.

[34] Kargosha K, Khanmohammadi M, Ghadiri M. Vapour phase Fourier transform infrared spectrometric determination of thiourea. The Analyst 2001;126(8):1432-1435.

[35] Shahzad U, Marwani H, Rabbee M, Alfaifi S, Alzahrani K, Khan M, Rahman M. Efficient sensitive detection of nitrite with Binary Y/Fe-modified multiwalled carbon nanotube nanocomposite by electrochemical approaches. Materials Chemistry and Physics 2024;328:130000.

[36] Saeed M, Marwani H, Shalauddin M, Alfaifi S, Akhter S, Alzahrani K, Jefrey Basirun W, Rahman M. Sensitive detection of unsafe nitrite chemical based on GO@Fe2O3/Y2O3 nanocomposite by electrochemical approach for environmental assessment. Journal of Industrial and Engineering Chemistry 2025;144:552-564.

[37] Jodan I, Wantala K, Amini N, Shahmoradi B, Ghaslani M, Lee S, Yang J, Puttaiah S. Fabrication of a sensitive electrochemical sensor based on Ag nanoparticles and alizarin yellow polymer: Application to the detection of an environmental pollutant thiourea. Korean Journal of Chemical Engineering 2020;37(9):1609-1615.

[38] Rashed M, Ahmed J, Faisal M, Alsareii S, Jalalah M, Harraz F. Highly sensitive and selective thiourea electrochemical sensor based on novel silver nanoparticles/chitosan nanocomposite. Colloids and Surfaces A: Physicochemical and Engineering Aspects 2022;644:128879.

[39] Khaleque M, Hossain M, Ali M, Bacchu M, Saad Aly M, Khan M. Nanostructured wearable electrochemical and biosensor towards healthcare management: a review. RSC Advances 2023;13(33):22973-22997.

[40] Patel LD. Phytopharmacological properties of Randia dumetorum as a potential medicinal tree: an overview. Journal of Applied Pharmaceutical Science 2011:24-6.

[41] Panáček A, Kvítek L, Prucek R, Kolář M, Večeřová R, Pizúrová N, Sharma V, Nevěčná T, Zbořil R. Silver Colloid Nanoparticles: Synthesis, Characterization, and Their Antibacterial Activity. The Journal of Physical Chemistry B 2006;110(33):16248-16253.

[42] Sharma V, Yngard R, Lin Y. Silver nanoparticles: Green synthesis and their antimicrobial activities. Advances in Colloid and Interface Science 2009;145(1-2):83-96.

[43] Garza-Navarro M, Aguirre-Rosales J, Llanas-Vázquez E, Moreno-Cortez I, Torres-Castro A, González-González V. Totally Ecofriendly Synthesis of Silver Nanoparticles from Aqueous Dissolutions of Polysaccharides. International Journal of Polymer Science 2013;2013:1-8.

[44] Kajani A, Bordbar A, Zarkesh Esfahani S, Khosropour A, Razmjou A. Green synthesis of anisotropic silver nanoparticles with potent anticancer activity using Taxus baccata extract. RSC Adv. 2014;4(106):61394-61403.

[45] Raveendran P, Fu J, Wallen S. Completely “Green” Synthesis and Stabilization of Metal Nanoparticles. Journal of the American Chemical Society 2003;125(46):13940-13941.

[46] Ajitha B, Ashok Kumar Reddy Y, Sreedhara Reddy P. Biosynthesis of silver nanoparticles using Plectranthus amboinicus leaf extract and its antimicrobial activity. Spectrochimica Acta Part A: Molecular and Biomolecular Spectroscopy 2014;128:257-262.

[47] Kamble PS, Shinde PB, Patil SA. Green Synthesis of Silver nanoparticles from Solanum torvum and its Antibacterial Potential. Int. J. Innov. Sci. Res. Technol. 2022; 7:1176-86.

[48] Anandalakshmi K, Venugobal J, Ramasamy V. Characterization of silver nanoparticles by green synthesis method using Pedalium murex leaf extract and their antibacterial activity. Applied Nanoscience 2015;6(3):399-408.

[49] Dare E, Oseghale C, Labulo A, Adesuji E, Elemike E, Onwuka J, Bamgbose J. Green synthesis and growth kinetics of nanosilver under bio-diversified plant extracts influence. Journal of Nanostructure in Chemistry 2014;5(1):85-94.

[50] Lee JW, Mho SI, Yeo IH. Flow injective determination of thiourea by amperometry. Bulletin-Korean Chemical Society 1994;15:1038-42.

[51] Manea F, Radovan C, Schoonman J. Amperometric determination of thiourea in alkaline media on a copper oxide–copper electrode. Journal of Applied Electrochemistry 2006;36(10):1075-1081.

[52] Khaleque M, Ali M, Bacchu M, Mamun M, Hossain M, Hossain M, Aly Saad Aly M, Khan M. Zinc oxide nanorod/rutin modified electrode for the detection of Thiourea in real samples. Heliyon 2023;9(10):e20676.

[53] Shahzad U, Marwani H, Akhter S, Shalauddin M, Alfaifi S, Basirun W, Rabbee M, Rahman M. Y/Co-MWCNT nanocomposite conjugated Nafion modified glassy carbon electrode for sensitive detection of thiourea chemical by electrochemical approach. Surfaces and Interfaces 2024;55:105466.